Centrifuge-Based Fluidic Platforms

JIM V. ZOVAL AND MARC J. MADOU

Invited Paper

In this paper, centrifuge-based microfluidic platforms are reviewed and compared with other popular microfluidic propulsion methods. The underlying physical principles of centrifugal pumping in microfluidic systems are presented and the various centrifuge fluidic functions such as valving, decanting, calibration, mixing, metering, heating, sample splitting, and separation are introduced. Those fluidic functions have been combined with analytical measurement techniques such as optical imaging, absorbance and fluorescence spectroscopy and mass spectrometry to make the centrifugal platform a powerful solution for medical and clinical diagnostics and high-throughput screening (HTS) in drug discovery. Applications of a compact disk (CD)-based centrifuge platform analyzed in this paper include two-point calibration of an optode-based ion sensor, an automated immunoassay platform, multiple parallel screening assays, and cellular-based assays. The use of modified commercial CD drives for high-resolution optical imaging is discussed as well. From a broader perspective, we compare technical barriers involved in applying microfluidics for sensing and diagnostics as opposed to applying such techniques to HTS. The latter poses fewer challenges and explains why HTS products based on a CD fluidic platform are already commercially available, while we might have to wait longer to see commercial CD-based diagnostics.

Keywords*—*BioMEMS, centrifugal fluidics, compact disk (CD), diagnostics, high-throughput screening (HTS), microfluidics.

I. INTRODUCTION

Once it became apparent that individual chemical or biological sensors used in complex samples would not attain the hoped-for sensitivity or selectivity, wide commercial use became severely hampered and sensor arrays and sensor instrumentation were proposed instead. It was projected that by using orthogonal sensor array elements (e.g., in electronic noses and tongues), selectivity would be improved dramatically [1]. It was envisioned that intrumentation would reduce matrix complexities through filtration, separation, and concentration of the target compound while at the same time ameliorating selectivity and sensitivity of the overall system by frequent recalibration and washing of the sensors. With microfluidics, the miniaturization of analytical equipment may potentially alleviate the shortcomings associated with large and expensive instrumentation through the reduction in reagent volumes, favorable scaling properties of several important instrument processes (basic theory of hydrodynamics and diffusion predicts faster heating and cooling and more efficient chromatographic and electrophoretic separations in miniaturized equipment), and batch fabrication, which may enable low-cost, disposable instruments to be used once and then thrown away to prevent sample contamination [2]. Micromachining [microelectromechanical systems (MEMS)] might also allow cofabrication of many integrated functional instrument blocks. Tasks that are now performed in a series of conventional bench-top instruments could then be combined into one unit, reducing labor and minimizing the risk of sample contamination.

Today it appears that sensor array development in electronic noses and tongues has slowed down because of the lack of highly stable chemical and biological sensors: too frequent recalibration of the sensors and relearning of the pattern recognition software is putting a damper on the original enthusiasm for this sensor approach. In the case of miniaturization of instrumentation through the application of microfluidics, progress was made in the development of platforms for high-throughput screening (HTS) as evidenced by new products introduced by, for example, Caliper and Tecan Boston, Medford, MA [3], [4]. In contrast, progress with miniaturized analytical equipment remains limited. There have been platforms developed for a limited number of human and veterinary diagnostic tests that do not require complex fluidic design—for example, Abaxis [5]. In this paper we are, in a narrow sense, summarizing the state of the art of compact disk (CD)-based microfluidics; in a broader sense, we are comparing the technical barriers involved in applying microfluidics to sensing and diagnostics as opposed to applying such techniques to HTS. It will quickly become apparent that the former poses the more severe technical challenges; as a result, the promise of lab on a chip has not been fulfilled yet.

Manuscript received May 5, 2003; revised July 31, 2003.

J. V. Zoval is with the Department of Mechanical and Aerospace Engineering, University of California, Irvine, CA 92697 USA (e-mail: jzoval@uci.edu).

M. J. Madou is with the Department of Mechanical and Aerospace Engineering and the Department of Biomedical Engineering, University of California, Irvine, Irvine, CA 92697 USA (e-mail: mmadou@uci.edu).

Digital Object Identifier 10.1109/JPROC.2003.820541

Table 1
Comparison of Microfluidics Propulsion Techniques

	Fluid Propulsion Mechanism			
Comparison	Centrifuge	Pressure	Acoustic	Electrokinetic
Valving solved ?	Yes for liquids no for vapor	Yes for liquids and vapor	No solution shown yet for liquid or vapor	Yes for liquids, no for vapor
Maturity	Products available	Products available	Research	Products available
Propulsion force influenced by	Density and viscosity	Generic	Generic	pH, ionic strength
Power source	Rotary motor	Pump, Mechanical roller	5 to 40 V	10 kV
Materials	Plastics	Plastics	Piezoelectrics	Glass, plastics
Scaling	L^3	L^3	L^2	L^2
Flow rate	From less than 1nL/sec to greater than 100 l/sec	Very wide range (less than nL/sec to L/sec)	20 l/sec	0.001-1 l/sec
General remarks	Inexpensive CD drive, mixing is easy, most samples possible (including cells). Better for diagnostics.	Standard technique. Difficult to miniaturize and multiplex.	Least mature of the four techniques. Might be too expensive. Better for smallest samples.	Mixing difficult. High voltage source is dangerous and many parameters influence propulsion, better for smallest samples (HTS)

II. Why Centripetal Force for Fluid Propulsion?

There are various technologies for moving small quantities of fluids or suspended particles from reservoirs to mixing and reaction sites, to detectors, and eventually to waste or to the next instrument. Methods to accomplish this include syringe and peristaltic pumps, electrochemical bubble generation, acoustics, magnetics, dc and ac electrokinetics, centrifuge, etc. In Table 1 we compare four of the more important and promising fluid propulsion means [6]. The pressure that mechanical pumps have to generate to propel fluids through capillaries is higher the narrower the conduit. Pressure and centripetal force are both volume-dependent forces, which scale as L^3 (in this case L is the characteristic length corresponding to the capillary diameter). Piezoelectric, electroosmotic, electrowetting, and electrohydrodynamic (EHD) pumping (the latter two are not shown in Table 1) all scale as surface forces (L^2), which represent more favorable scaling behavior in the micro domain (propulsion forces scaling with a lower power of the critical dimension become more attractive in the micro domain) and lend themselves better to pumping in smaller and longer channels. In principle, this should make pressure- and centrifuge-based systems less favorable but other factors turn out to be more decisive; despite better scaling of the nonmechanical pumping approaches in Table 1, almost all biotechnology equipment today remain based on traditional external syringe or peristaltic pumps. The advantages of this approach are that it relies on well-developed, commercially available components and that a very wide range of flow rates is attainable. Although integrated micromachined pumps based on two one-way valves may achieve a precise flow control on the order of 1 μl/min with fast response, high sensitivity, and negligible dead volume, these pumps generate only modest flow rates and low pressures, and consume a large amount of chip area and considerable power.

Acoustic streaming is a constant (dc) fluid motion induced by an oscillating sound field at a solid/fluid boundary. A disposable fluidic manifold with capillary flow channels can simply be laid on top of the acoustic pump network in the reader instrument. The method is considerably more complex to implement than electroosmosis, but the insensitivity of acoustic streaming to the chemical nature of the fluids inside the fluidic channels and its ability to mix fluids make it a potentially viable approach. A typical flow rate measured for water in a small metal pipe lying on a piezoelectric plate is 0.02 cc/s at 40 V, peak to peak [7]. Today acoustic streaming as a propulsion mechanism remains in the research stage.

Electroosmotic pumping (dc electrokinetics) in a capillary does not involve any moving parts and is easily implemented. All that is needed is a metal electrode in some type of a reservoir at each end of a small flow channel. Typical electroosmotic flow velocities are on the order

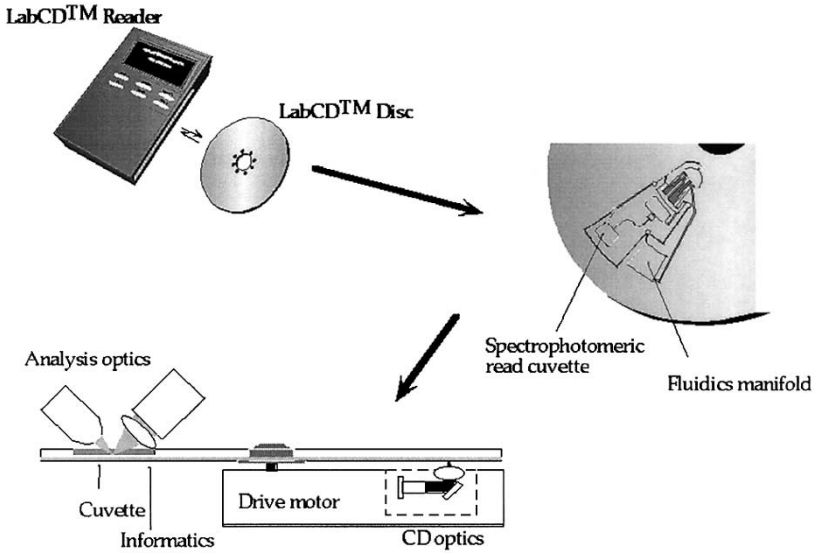

Fig. 1. LabCD instrument and disposable disk. Here, the analytical result is obtained through reflection spectrophotometry.

of 1 mm/s with a 1200-V/cm applied electric field. For example, in free-flow capillary electrophoresis work by Jorgenson, electroosmotic flow of 1.7 mm/s was reported [8]. This is fast enough for most analytical purposes. Harrison *et al.* achieved electroosmotic pumping with flow rates up to 1 cm/s in 20-μm capillaries that were micromachined in glass [9]. They also demonstrated the injection, mixing, and reaction of fluids in a manifold of micromachined flow channels without the use of valves. The key aspect for tight valving of liquids at intersecting capillaries in such a manifold is the suppression of convective and diffusion effects. The authors demonstrated that these effects can be controlled by the appropriate application of voltages to the intersecting channels simultaneously. Some disadvantages of electroosmosis are the required high voltage (1–30-kV power supply) and direct electrical-to-fluid contact with resulting sensitivity of flow rate to the charge of the capillary wall and to the ionic strength and pH of the solution. It is, consequently, more difficult to make it into a generic propulsion method. For example, liquids with high ionic strength cause excessive Joule heating; it is, therefore, difficult or impossible to pump biological fluids such as blood and urine.

Using a rotating disk, centrifugal pumping provides flow rates ranging from less than 10 nL/s to greater than 100 μL/s depending on disk geometry, rotational rate (r/min), and fluid properties (see Fig. 1) [10]. Pumping is relatively insensitive to physicochemical properties such as pH, ionic strength, or chemical composition (in contrast to ac and dc electrokinetic means of pumping). Aqueous solutions, solvents [e.g., dimethyl sulfoxide (DMSO)], surfactants, and biological fluids (blood, milk, and urine) have all been pumped successfully. Fluid gating, as we will describe in more detail, is accomplished using "capillary" valves in which capillary forces pin fluids at an enlargement in a channel until rotationally induced pressure is sufficient to overcome the capillary pressure (at the so-called burst frequency) or by hydrophobic methods. Since the types and amounts of fluids one can pump on a centrifugal platform span a greater dynamic range than for electrokinetic and acoustic pumps, this approach seems more amenable to sample preparation tasks than electrokinetic and acoustic approaches. Moreover, miniaturization and multiplexing are quite easily implemented. A whole range of fluidic functions, including valving, decanting, calibration, mixing, metering, sample splitting, and separation, can be implemented on this platform; analytical measurements may be electrochemical, fluorescent, or absorption based, and informatics embedded on the same disk could provide test-specific information.

A most important deciding factor in choosing a fluidic system is the ease of implementing valves; the method that most elegantly solves the valving issue is already commercially accepted, even if the scaling is not the most favorable, namely, the use of traditional pumps. In traditional pumps, two one-way valves form a barrier for both liquids and vapors. In the case of the microcentrifuge, valving is accomplished by varying rotation speed and capillary diameter. Thus, there is no real physical valve required for stopping water flow, but as in the case of acoustic and electrokinetic pumping, there is no simple means to stop vapors from spreading over the whole fluidic platform. If liquids need to be stored for a long time on the disposable, as often is the case for use in sensing and diagnostics, valves must be barriers for both liquid and vapor. Some timid attempts at implementing vapor barriers on the CD will be reported in this paper.

From the preceding comparison of fluidic propulsion methods for sensing and diagnostic applications, centrifugation in fluidic channels and reservoirs crafted in a CD-like plastic substrate, as shown in Fig. 1, constitutes an attractive fluidic platform.

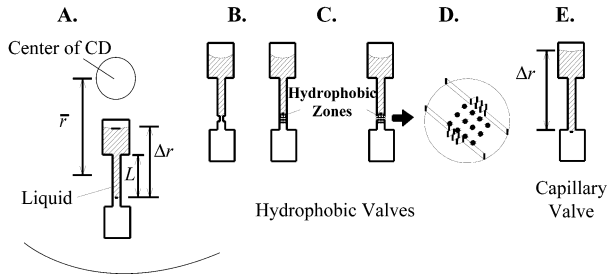

Fig. 2. Schematic illustrations for the description of CD microfluidics. (A) Two reservoirs connected by a microfluidic chamber. (B) Hydrophobic valve made by a constriction in a chamber made of hydrophobic material. (C) Hydrophobic valve made by the application of hydrophobic material to a zone in the channel. (D) Hydrophobic channel made by the application of hydrophobic material to a zone in a channel made with structured vertical walls (see inset). (E) Capillary valve made by a sudden expansion in channel diameter such as when a channel meets a reservoir.

III. CD or Microcentrifuge Fluidics

A. How It Works

CD fluid propulsion is achieved through centrifugally induced pressure and depends on rotation rate, geometry and location of channels and reservoirs, and fluid properties. Madou *et al.* [11] and Duffy *et al.* [10] characterized the flow rate of aqueous solutions in fluidic CD structures and compared the results to simple centrifuge theory. The average velocity of the liquid U from centrifugal theory is given as

$$U = D_h^2 \rho \omega^2 \bar{r} \Delta r / 32 \mu L \tag{1}$$

and the volumetric flow rate (Q) as

$$Q = UA \tag{2}$$

where D_h is the hydraulic diameter of the channel (defined as $4A/P$, where A is the cross-sectional area and P is the wetted perimeter of the channel), ρ is the density of the liquid, ω is the angular velocity of the CD, $\bar{r}$ is the average distance of the liquid in the channels to the center of the disk, Δr is the radial extent of the fluid, μ is the viscosity of the solution, and L is the length of the liquid in the capillary channel [see also Fig. 2(A)]. Flow rates, ranging from 5 nL/s to >0.1 mL/s, have been achieved by various combinations of rotational speeds (from 400 to 1600 r/min), channel widths (20–500 μm), and channel depths (16–340 μm). The experimental flow rates were compared to rates predicted by the theoretical model and exhibited an 18.5% coefficient of variation. The authors note that experimental errors in measuring the highest and lowest flow rates made for the largest contribution to this coefficient of variation. The absence of systematic deviation from theory validates the model for describing flow in microfluidic channels under centripetal force. Duffy *et al.* [10] measured flow rates of water, plasma, bovine blood, three concentrations of hematocrit, urine, DMSO, and polymerase chain reaction (PCR) products, and report that centrifugal pumping is relatively insensitive to such physiochemical properties as ionic strength, pH, conductivity, and the presence of various analytes, noting good agreement between experiment and theory for all the liquids.

IV. Some Simple Fluidic Function Demonstrated on a CD

A. Mixing of Fluid

In the work by Madou *et al.* [11] and Duffy *et al.* [10], different means to mix liquids were designed, implemented, and tested. Observations of flow velocities in narrow channels on the CD enabled Reynolds numbers (R_e) calculations establishing that the flow remained laminar in all cases. Even in the largest fluidic channels tested R_e was <100, well below the transition regime from laminar to turbulent flow ($R_e \sim 2300$) [12]. The laminar flow condition necessitates mixing by simple diffusion or by creating special features on the CD that do enable advection or turbulence. In one scenario, fluidic diffusional mixing was implemented by emptying two microfluidic channels together into a single long, meandering fluidic channel. Proper design of channel length and reagent reservoirs allowed for stoichiometric mixing in the meandering channel by maintaining equal flow rates of the two streams joining into the mixing channel. Concentration profiles may be calculated from the diffusion rates of the reagents and the time required for the liquids to flow through the tortuous path. Mixing can also be achieved by chaotic advection [6]. Chaotic advection is a result of the rapid distortion and elongation of the fluid/fluid interface, increasing the interfacial area where diffusion occurs, which increases the mean values of the diffusion gradients that drive the diffusion process; one may call this process an enhanced diffusional process. In addition to simple and enhanced diffusional processes, one can create turbulence on the CD by emptying two narrow streams to be mixed into a common chamber. The streams violently splash against a common chamber wall causing their effective mixing (no continuity of the liquid columns is required on the CD as opposed to the case of electrokinetics platforms where a broken-up liquid column would cause a voltage overload).

B. Valving

Valving is a most important function in any type of fluidic platform. Both hydrophobic and capillary valves have been integrated into the CD platform [10], [11], [13]–[23]. Hydrophobic valves feature an abrupt decrease in the hydrophobic channel cross section, i.e., a hydrophobic surface prevents further fluid flow [Fig. 2(B)–(D)]. In contrast, in capillary valves [Fig. 2(E)], liquid flow is stopped by a capillary pressure barrier at junctions where the channel diameter suddenly expands.

1) Hydrophobic Valving: The pressure drop in a channel with laminar flow is given by the Hagen–Poiseuille equation [12]

$$\Delta P = \frac{12 L \mu Q}{w h^3} \tag{3}$$

where L is the microchannel length, μ is the dynamic viscosity, Q is the flow rate, and w and h are the channel width

and height. The required pressure to overcome a sudden narrowing in a rectangular channel is given by [6]

$$\Delta P = 2\sigma_l \cos(\theta_c)\left[\left(\frac{1}{w_1}\right)+\left(\frac{1}{h_1}\right)\right] - \left[\left(\frac{1}{w_2}\right)+\left(\frac{1}{h_2}\right)\right] \quad (4)$$

where σ_l is the liquid's surface tension, θ_c is the contact angle, w_1 and h_1 are the width and height of the channel before the restriction, and w_2 and h_2 are the width and height after the restriction. In hydrophobic valving, in order for liquid to move beyond these pressure barriers, the CD must be rotated above a critical speed, at which point the centripetal forces exerted on the liquid column overcome the pressure needed to move past the valve.

Ekstrand *et al.* [13] used hydrophobic valving on a CD to control discrete sample volumes in the nanoliter range with centripetal force. Capillary forces draw liquid into the fluidic channel until there is a change in the surface properties at the hydrophobic valve region. The valving was implemented as described schematically in Fig. 2(C). Tiensuu *et al.* [14] introduced localized hydrophobic areas in CD microfluidic channels by ink-jet printing of hydrophobic polymers onto hydrophilic channels. In this work, hydrophobic lines were printed onto the bottom wall of channels with both unstructured [Fig. 2(C)] and structured [Fig. 2(D)] vertical channel walls. Several channel width to depth ratios were investigated. The CDs were made by injection molding of polycarbonate. The CDs were subsequently rendered hydrophilic by oxygen plasma treatment, and then ink-jet printing was used for the introduction of the hydrophobic polymeric material at the valve position. The parts were capped with poly(dimethylsiloxane) (PDMS) to form the fourth wall of the channel. In testing of nonstructured channels (without sawtooth pattern), there were no valve failures for 300- and 500-μm-wide channels but some failures for the 100-μm channels, however, in structured vertical walls (with sawtooth patterns), there were no valve failures. The authors attribute the better results of the structured vertical walls to both the favorable distribution of hydrophobic polymer within the channel and the sharper sidewall geometry to be wetted (the side walls are hydrophilic since the printed hydrophobic material is only on the bottom of the channel) compared to the nonstructured vertical channel walls.

2) Capillary Valving: Capillary valves have been implemented frequently on CD fluidic platforms [10], [11], [15]–[18], [21], [22]. The physical principle involved is based on the surface tension, which develops when the cross section of a hydrophilic capillary expands abruptly as illustrated in Fig. 2(E). As shown in this figure, a capillary channel connects two reservoirs, and the top reservoir (the one closest to the center of the CD) and the connecting capillary is filled with liquid. For capillaries with axisymetric cross sections, the maximum pressure at the capillary barrier expressed in terms of the interfacial free energy [16] is given by

$$P_{\rm cb} = 4\gamma_{\rm al}\sin\theta_c/D_h \quad (5)$$

where $\gamma_{\rm al}$ is the surface energy per unit area of the liquid–air interface, θ_c is the equilibrium contact angle, and D_h is the hydraulic diameter. Assuming low liquid velocities, the flow dynamics may be modeled by balancing the centripetal force and the capillary barrier pressure [see (5)]. The liquid pressure at the meniscus, from the centripetal force acting on the liquid, can be described as follows:

$$P_m = \rho\omega^2\bar{r}\Delta r \quad (6)$$

where, ρ is the density of the liquid, ω is the angular velocity, $\bar{r}$ is the average distance from the liquid element to the center of the CD, and Δr is the radial length of the liquid sample [Fig. 2(A) and (E)]. Liquid will not pass a capillary valve as long as the pressure at the meniscus (P_m) is less than or equal to the capillary barrier pressure $P_{\rm cb}$). Kellogg and coworkers [16] named the point at which P_m equals $P_{\rm cb}$, the *critical burst condition* and the rotational frequency at which it occurs they called the *burst frequency*. Experimental values of critical burst frequencies versus channel geometry, for rectangular cross sections over a range of channel sizes, show good agreement with simulation over the entire range of diameters studied. Since these simulations did not assume an axisymetric capillary with a circular contact line and a diameter D_h, the meniscus contact line may be a complex shape. Burst frequencies were shown to be cross-section dependent for equal hydraulic diameters. The theoretical burst frequency equation was modified as follows to account for variation of channel cross section:

$$\rho\omega^2\bar{r}\Delta r < 4\gamma_{\rm al}\sin\theta_c/(D_h)^n \quad (7)$$

where $n = 1.08$ for an equilateral triangular cross section and $n = 1.14$ for a rectangular cross section. For "pipe flow" (circular cross section), an additional term is used in the burst frequency expression

$$\rho\omega^2\bar{r}\Delta r < 4\gamma_{\rm al}\sin\theta_c/(D_h) + \gamma_{\rm al}\sin\theta_c(1/D_h - 1/D_0) \quad (8)$$

where the empirically determined constant $D_0 = 40$ μm. The physical reason for the additional "pipe flow" term, used to get a fit to the simulation results, is not well understood at this time.

Duffy *et al.* [10] modeled capillary valving by balancing the pressure induced by the centripetal force ($\rho\omega^2\bar{r}\Delta r$) at the exit of the capillary with the pressure inside the liquid droplet being formed at the capillary outlet and the pressure required to wet the chamber beyond the valve. The pressure inside a droplet is given by the Young–Laplace equation [24]

$$\Delta P = \gamma(1/R_1 + 1/R_2) \quad (9)$$

where γ is the surface tension of the liquid and R_1 and R_2 are the meniscus radii of curvature in the x and y dimensions of the capillary cross section. In the case of small circular capillary cross sections with spherical droplet shapes, $R_1 =$

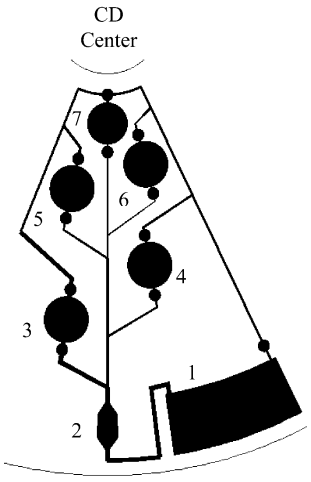

Fig. 3. Schematic illustration of the microfluidic structure employed for the ion-selective optode CD platform. The fluidic structure contains five solution reservoirs (numbered 1–5), a detection chamber (6), and a waste reservoir (7). Reservoirs 1 and 3 contain the first and second calibrant, respectively; reservoirs 2 and 4 contain wash solutions; and reservoir 5 contains the sample. Upon increasing rotation rates, calibrant 1, wash 1, calibrant 2, rinse 2, and then sample were serially gated into the optical detection chamber. Absorption of the calibrants and sample was measured.

$R_2 \cong$ channel cross-section radius, and (9) can be rewritten as

$$\Delta P = 4\gamma/D_h. \tag{10}$$

On this basis Duffy *et al.* [10] derived a simplified expression for the critical burst frequency (ω_c) as

$$\rho\omega_c^2\bar{r}\Delta r = a(4\gamma/D_h) + b \tag{11}$$

with the first term on the right representing the pressure inside the liquid droplet being formed at the capillary outlet scaled by a factor a (for nonspherical droplet shapes) and the second term on the right b representing the pressure required to wet the chamber beyond the valve. The b term depends on the geometry of the chamber to be filled and the wettability of its walls.

A plot of the centripetal pressure $(\rho\omega_c^2\bar{r}\Delta r)$ at which the burst occurs versus $1/D_h$ was linear, as expected from (11), with a 4.3% coefficient of variation. The authors note a potential limitation with capillary valves due to the fact that liquids with low surface tension tend to wet the walls of the chamber at the capillary valve opening resulting in the inability to gate the flow. The b term in (11) is beneficial in gating flow unless the surface walls at the abrupt enlargement of the capillary valve are so hydrophilic that the liquid is drawn past the valve and into the reservoir.

Madou *et al.* [17], [18] have designed a CD to sequentially valve fluids through a monotonic increase of rotational rate with progressively higher "burst" frequencies. The CD, shown in Fig. 3, was designed to carry out an assay for ions based on an optode-based detection scheme. The CD design employed five serial capillary valves opening at different times as actuated by rotational speed. Results show good agreement between the observed and the calculated burst frequencies (see later).

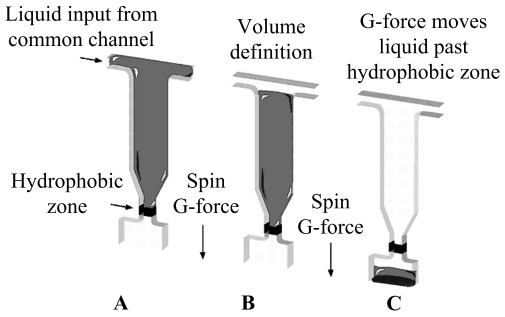

Fig. 4. Schematic illustration of liquid metering. (A) The common distribution channel and liquid metering reservoirs are filled (by capillary forces) with a reagent to be metered. Liquid entering the reservoir does not pass the hydrophobic zone (valve) because of surface tension forces. (B) The CD is rotated at a rate that supplies enough centripetal force to empty the common distribution but not enough to force the liquid through the hydrophobic zone. The volume of the fluid metered is determined by the volume of the reservoir. (C) A further increase in the rotational speed provides enough force to move the well defined volume of solution past the hydrophobic valve. (With kind permission: Application Report 101, Gyrolab MALDI SP1, Gyros AB, Uppsala, Sweden [20].)

It is very important to realize that the valves we mentioned thus far constitute liquid barriers and that they are not barriers for vapors. Vapor barriers must be implemented in any fluidic platform where reagents need to be stored for long periods of time. This is especially important for a disposable diagnostic assay platform. A multimonth, perhaps multiyear, shelf life would require vapor locks in order to prevent reagent solutions from drying or liquid evaporation and condensation in undesirable areas of the fluidic pathway. Tecan-Boston did investigate vapor-resistant valves made of wax that was melted to actuate the valve opening [25].

C. Volume Definition (Metering) and Common Distribution Channels

The CD centrifugal microfluidic platform enables very fine volume control (or metering) of liquids. Precise volume definition is one of the important functions, necessary in many analytical sample processing protocols, which has been added, for example, to the fluidic design in the Gyrolab MALDI SP1 CD [20]. In this CD, developed for matrix-assisted laser desorption ionization (MALDI) sample preparation, a common distribution channel feeds several parallel individual sample preparation fluidic structures (Fig. 4). Reagents are introduced by the capillary force exerted by the hydrophilic surfaces into the common channel and defined volume (200 nl) chambers until a hydrophobic valve stops the flow. When all of the defined-volume chambers are filled, the CD is spun at a velocity large enough to move the excess liquid from the common channel into the waste. Although there is sufficient centripetal force to empty the common channel, the velocity is not so high as to allow liquid to move past the hydrophobic valve and the well-defined volume chambers remain filled. These precisely defined volumes can be introduced into the subsequent fluidic structures by increasing the CD angular momentum until the centripetal force allows the liquid to move past the hydrophobic barriers.

D. Packed Columns

Many commercial products are now available that use conventional centrifuges to move liquid, in a controlled manner, through a chromatographic column. One example is the Quick Spin protein desalting column (Roche Diagnostics Corp, Indianapolis, IN), based on the size exclusion principle. There is an obvious fit for this same type of separation experiment to be carried out on a CD fluidic device (we sometimes refer to the CD platform as a smart, miniaturized centrifuge). Affinity chromatography has been implemented in the fluidic design of the Gyrolab MALDI SP1 CD [20]. A reverse phase chromatography column material (SOURCE15 RPC) is packed in a microfluidic channel and protein is adsorbed on the column from an aqueous sample as it passes through the column under centrifugally controlled flow rates. A rinse solution is subsequently passed through the column, and finally an elution buffer is flowed through to remove the protein and carry it into the fluidic system for further processing. The complete Gyrolab MALDI SP1 CD is discussed later.

V. CD Applications

A. Two-Point Calibration of an Optode-Based Detection System

A CD-based system with ion-selective optode detection and a two-point-calibration structure for the accurate detection of a wide variety of ions was developed. [15], [17], [18] The microfluidic architecture, depicted in Fig. 3, is composed of channels, five solution reservoirs, a chamber for colorimetric measurement of the optode membrane, and a waste reservoir, all manufactured onto a poly(methyl methacrylate) disk. Ion-selective optode membranes, composed of plasticized poly(vinyl chloride) impregnated with an ionophore, a chromoionophore, and a lipophilic anionic additive, were cast, with a spin-on device, onto a support layer and then immobilized on the disk. With this system, it is possible to deliver calibrant solutions, washing buffers, and "unknown" solutions (e.g., saliva, blood, urine, etc.) to the measuring chamber where the optode membrane is located. Absorbance measurements on a potassium optode indicate that optodes immobilized on the platform exhibit the theoretical absorbance response. Samples of unknown concentration can be quantified to within 3% error by fitting the response curve for a given optode membrane using an acid (for measuring the signal for a fully protonated chromoionophore), a base (for fully deprotonated chromoionophore), and two standard solutions. Further, the ability to measure ion concentrations employing one standard solution in conjunction with acid and base, and with two standards alone were studied to delineate whether the current architecture could be simplified. Finally, the efficacy of incorporating washing steps into the calibration protocol was investigated.

This work was further extended to include anion-selective optodes and fluorescence rather than absorbance detection [17]. Furthermore, in addition to employing a standard excitation source where a fiber optic probe is coupled to a lamp, LASER diodes were evaluated as excitation sources to enhance the fluorescence signal.

VI. CD Platform for Enzyme-Linked Immunosorbant Assays (ELISA)

The automation of immunoassays on microfluidic platforms presents multiple challenges because of the high number of fluidic processes and the many different liquid reagents involved. Often there is also the need for highly accurate quantitative results at extremely low concentration and care must be taken to prevent nonspecific binding of reporter enzymes and to deliver well defined volumes of reagents consistently. An enzyme-linked immunosorbant assay (i.e., ELISA) is one of the most common immunoassay methods and is often carried out in microtiter plates using labor-intensive manual pippetting techniques. Recently, Lee *et al.* [21] have implemented an automated enzyme-linked immunosorbant assay on the CD platform. This group used a five-step flow sequence in the same CD design illustrated in Fig. 3. A capture antibody (antirat IgG) was applied to the detection reservoir (reservoir 2 in Fig. 3) by adsorption to the PMMA CD surface, then the surface was blocked to prevent nonspecific binding. Antigen/sample (rat IgG), wash solution, a second antibody, and substrate solutions were loaded into reservoirs 3–7 (Fig. 3), respectively. Using capillary valving techniques, the sample and reagents were pumped, one at a time, through the detection chamber. First, the sample was introduced for antibody–antigen binding (reservoir 3), then a wash solution (reservoir 4), then an enzyme-labeled secondary antibody (reservoir 5), then another wash solution (reservoir 6), and finally the substrate was added (reservoir 7). The U-shaped bend in the fluidic path allows the solutions to incubate in the capture zone/detection chamber until the next solution is released into the chamber. Detection of the fluorescence is performed after the substrate is introduced into the detection reservoir (reservoir 2). Endpoint measurements (completion of enzyme-substrate reaction) were made and compared to conventional microtiter plate methods using similar protocols. The CD ELISA platform was shown to have advantages such as lower reagent consumption, and shorter assay times, explained in terms of larger surface to volume ratios which favor diffusion limited processes. Since the reagents were all loaded into the CD at the same time, there was no need for manual operator interventions in between fluidic assay steps. The consistent control and repeatability of liquid propulsion removes experimental errors associated with inconsistent manual pippetting methods; for example, rinsing/washing can be carried out not only with equal volumes, but equal flow conditions.

VII. Multiple Parallel Assays

The ability to obtain simultaneous and identical flow rates, incubation times, mixing dynamics, and detection makes the CD an attractive platform for multiple parallel

assays. Kellogg *et al.* [10] reported on a CD system that performs multiple (48) enzymatic assays simultaneously by combining centrifugal pumping in microfluidic channels with capillary valving and colorimetric detection. The investigation of multiplexed parallel enzyme inhibitor assays are needed for HTS in diagnostics and in screening of drug libraries. For example, enzymatic dephosphorylation of colorless p-nitrophenol phosphate by alkaline phosphatase results in the formation of the yellow-colored p-nitrophenol, and inhibition of this reaction may be quantified by light absorption measurement. Theophylline, a known inhibitor of the reaction, was used as the model inhibitory compound in Kellogg *et al.*'s [10] feasibility study. A single assay element on the CD contains three reservoirs: one for the enzyme, one for the inhibitor, and one for the substrate. Rotation of the CD allows the enzyme and inhibitor to pass capillary valves, mix in a meandering 100-μm-wide channel, and then move to a point where flow is stopped by another capillary valve. A further increase in the rotational speed allows the enzyme/inhibitor mixture and substrate to pass through the next set of capillary valves, where they are mixed in a second meandering channel and emptied into an on-disk planar cuvette. The CD is slowed and absorption through each of the 48 parallel assay cuvettes is measured by reflectance, all in a period of 60 s, the entire fluidic process including measurement took about 3 min. The CDs were fabricated using PDMS replication techniques [26], with the addition of a white pigment to the PDMS polymerization for enhanced reflectivity in the colorimetric measurements. The flow rates and meandering channel widths were selected such that the diffusion rate would allow 90% mixing of the solutions.

The variation in performance between the individual fluidic CD structures was quantified by carrying out the same assay 45 times simultaneously on a CD. The background corrected absorbance was measured and the coefficient of variation in the assay was $\sim$3.2%. When the experiment was repeated on different disks the coefficient of variation ranged from 3% to 3.5%. Furthermore, variation of absorption across a single cuvette was less than 1%, confirming complete mixing. In experiments to show enzyme inhibition, 45 simultaneous reactions were carried out on the CD using fixed concentrations of enzyme and substrate and 15 concentrations of theophylline in triplicate and a complete isotherm was generated for the inhibition of alkaline phosphatase. The three remaining structures were used for calibration with known concentrations of p-nitrophenol. A dose response was seen over three logs of theophylline concentration in the range of 0.1 to 100 mM. The authors conclude that a large number of identical assays, with applications in rapid HTS, can be carried out on the CD platform simultaneously because of the symmetric force acting on the fluids in high-quality identical microfluidic structures and that detection was simplified by rotating all the reaction mixtures under a fixed detector. In later work [22], the same group has extended the number of assays to 96 per CD and has investigated fluorescent enzymatic assays.

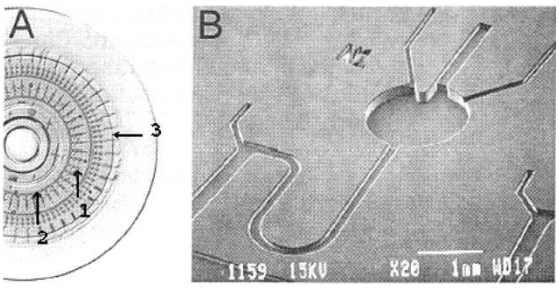

Fig. 5. Microfabricated cell culture CD. (A) The CD caries a number of cell growth chambers (1) radially arranged around a common distribution channel (2) and is sealed with a silicone cover (3). (B) SEM close-up of an individual cell growth chamber and microfluidic connections. (*Proc. Micro Total Analysis Systems 2000*, © 2000, pp. 249–252, N. Thomas, A. Ocklind, I. Blikstad, S. Griffiths, M. Kenrick, H. Derand, G. Ekstrand, C. Ellström, A. Larsson, and P. Anderson, "Integrated cell based assays in microfabricated disposable CD devices" [23], with kind permission of Kluwer Academic Publishers.)

VIII. Cellular-Based Assays on CD Platform

Cell-based assays are often used in drug screening [27] and rely on labor-intensive microtiter plate technologies. Microtiter plate methods may be difficult to automate without the use of large and expensive liquid handling systems, and they present problems with evaporation when scaled down to small volumes. Thomas *et al.* [23] reported on a CD platform-based automated adherent cell system. This adherent cell assays involved introducing the compounds to be screened to a cell culture, then determining if the cells were killed (cell viability assay).

Reagents for cell growth, rinsing, and viability staining were serially loaded into an annular common distribution chamber and centripetal force was used for reagent loading, exchange, and rinsing of the cell growth chamber (Fig. 5). Individual inlets are for the addition of compounds to be screened. The plastic channels [Fig. 5(B)] were capped with a PDMS sheet capable of fast gas transport in and out of the culture reservoirs.

HeLA, L929, CHO-M1, and MRC-5 cell lines were cultivated on the CD device. Cell viability assays were performed, on the CD, by removing the growth medium from the cells, washing the cells with PBS, and introducing a solution of the fluorescence assay reagents into the growth chamber. The LIVE/DEAD Viability Assay (Molecular Probes, Inc., Eugene, OR) uses a mixture of calcein green-fluorescent nucleic acid stain and the red-fluorescent nucleic acid stain ethidium. The assay performance is based on the differing abilities of the stains to penetrate healthy bacterial cells. The calcein green-fluorescent dye will label all cells, live or dead. The red red-fluorescent ethidium stain will only label cells with damaged membranes. The red stain causes a reduction in the green stain fluorescence when both dyes are present. When the appropriate mixture of green and red stains is used, cells with intact membranes will have a green fluorescence and cells with damaged membranes will have a red fluorescence. The background remains almost completely nonfluorescent (Fig. 6). All liquid transfers were carried out using centripetal force from CD rotation with angular frequencies

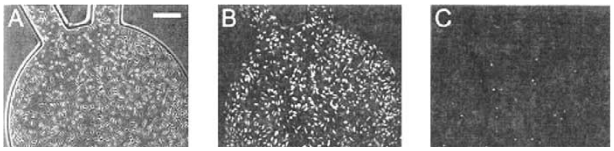

Fig. 6. L929 fibroblasts cultured for 48 h in CD growth chambers. (A) Phase contrast (scale bar 100 μm). (B) Epifluorescence image of calcein-stained viable cells. (C) Epifluorescence image of ethidium stained nonviable cells. (*Proc. Micro Total Analysis Systems 2000*, © 2000, pp. 249–252, N. Thomas, A. Ocklind, I. Blikstad, S. Griffiths, M. Kenrick, H. Derand, G. Ekstrand, C. Ellström, A. Larsson, and P. Anderson, "Integrated cell based assays in microfabricated disposable CD devices" [23], with kind permission of Kluwer Academic Publishers.)

between 200 and 600 r/min. Quantitative detection of multiple cell viability assays, within 30 s, was carried out by measurement of calcien fluorescence with a charge coupled device (CCD)-based fluorescence imaging system. These experimental results show linear fluorescence intensity across the range of 200–4000 cells and give an indication of the potential of this platform for miniaturized quantitative cell-based assays.

In the same work, the authors reported the results of experiments designed to investigate the effect on cells of using centripetal force to move liquids. The cells tested were shown to be compatible with centripetal forges of at least 600 $\times g$, much larger than the 50–100 $\times g$ needed for filling and emptying cell chambers. Furthermore, it was reported that cells grown in such devices appear to show the same cell morphology as cells grown under standard conditions.

In separate work done by our group in collaboration with NASA Ames *et al.* [28] the LIVE/DEAD BacLight Bacterial Viability Kit (Molecular Probes, Inc., Eugene, OR) has been integrated to a completely automated process on CD. Disposable and reusable CD structures, hardware, and software were developed for the LIVE/DEAD assay.

The CD design for assay automation must have the following functions or properties: contain separate reservoirs for each dye and the sample; retain those solutions in the reservoir until the disk is rotated at a certain velocity; evenly and completely mix the two dyes; evenly and completely mix the dye mixture with the sample containing the cells; and collect this final mixture in a reservoir with good optical properties. Two methods for quick fabrication of prototype CDs were used. One method used molded PDMS structures. In a second method, a dry film photoresist (DF 8130, Think & Tinker, Palmer Lake, CO) was laminated onto a 1-mm-thick polycarbonate disk with predrilled holes for sample introduction. The microfluidic pattern was made using a photolithographic pattern on the negative photoresist. The fluidic system was capped with a polycarbonate disk that had been laminated with an optical-quality pressure-sensitive adhesive (3M 8142, 3M, Minneapolis, MN). Fig. 7 shows the fluidic pattern for this assay. This pattern is based on the structure developed in a similar approach used to demonstrate multiple enzymatic assays on CD [10].

The dyes and sample were introduced into reservoir chambers using a pipette. The dyes fill the chamber stopping at a capillary valve (valve 1 in Fig. 7). Similarly, the sample

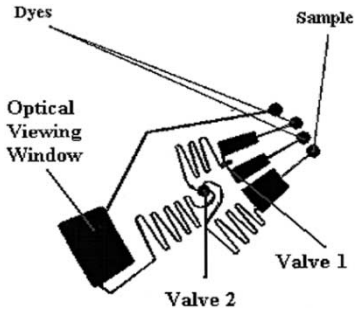

Fig. 7. Microfluidic pattern for LIVE/DEAD BacLight Bacterial Viability Assay. The dyes and sample are introduced into the reservoir chambers using a pipette. The dyes fill the chamber stopping at a capillary valve (valve 1). Similarly, the sample containing cells is introduced into the sample reservoir. The disk is rotated to a velocity of 800 r/min, the dyes are forced through the capillary valves, and they are mixed as they flow through the switchback turns of the microfluidic channels. Simultaneously, the sample passes from the reservoir into a fluid channel, where it meets the dye mixture at valve 2. The velocity of the disk is increased to 1600 r/min and the dye mixture and sample combine and mix in the switchback microfluidic path leading to the optical viewing window.

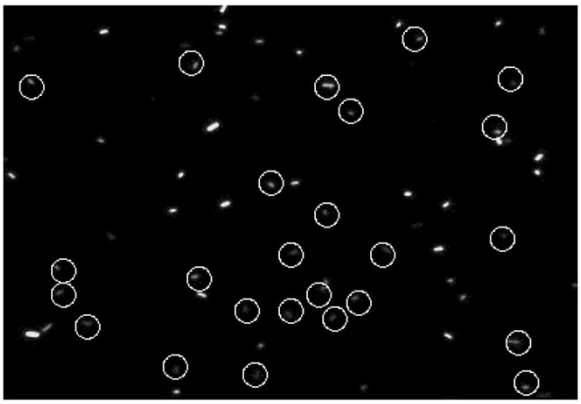

Fig. 8. Fluorescent microscopy overlaid images of red (circled cells) and green (uncircled cells) stained *E. coli* on CD from LIVE/DEAD BacLight Bacterial Viability Assay.

containing cells was introduced into the sample reservoir. Upon rotation, the dyes were forced through the capillary valves and were mixed as they flowed through the switchback turns of the microfluidic channels. Simultaneously, the sample passed from its reservoir into a fluid channel, where it met the dye mixture at valve 2 of Fig. 7. The velocity of the disk was increased, and the dye mixture and sample combine and mix in the switchback microfluidic path leading to the optical viewing window. The dye–sample mixture is allowed to incubate in the dark at room temperature for 5 min. The optical viewing chamber was imaged twice, once with optics for the green signal and then with optics for the red signal. A typical fluorescence microscopy image of an overlay of the red and green images of stained *E. coli* is shown in Fig. 8.

The instrument for disk rotation and fluorescence imaging (Fig. 9) used a programmable rotational motor for various velocities and acceleration/deceleration rates. The use of standard microscope objectives enabled the selection of magnification. An automatic focusing system was used.

Fig. 9. Left: Optical disk drive/imager with cover removed. Size of unit is made to fit in specific cargo bay of Space-Lab. Right: Zoom of microscope objectives and a disk loaded in the drive.

The light source was a mercury lamp, which used standard low-pass excitation filters for fluorescent excitation. A CCD camera was combined with standard emission filter cubes for imaging.

IX. Integrated Nucleic Acid Sample Preparation and PCR Amplification

Nucleic acid analysis is often facilitated by PCR and requires substantial sample preparation that, unless automated, is labor extensive. After the initial sample preparation step of cell lyses to release the DNA/RNA, a step must be taken to prevent PCR inhibitors, usually certain proteins such as hemoglobin, from entering into the PCR thermocyle reaction. This can be done by further purification methods such as precipitation and centrifugation, solid phase extraction, or by denaturing the inhibitory proteins. Finally, the sample must be mixed with the PCR reagents followed by thermocyling, a process that presents difficulty in a microfluidic environment because of the relatively high temperatures (up to 95 °C) required. In a small-volume microfluidic reaction chamber, the liquid will be easily evaporated unless care is taken to prevent vapor from escaping.

Kellogg *et al.* [22] combine sample preparation with PCR on the CD. The protocol involves the following steps: 1) mixing raw sample (5 μL of dilute whole bovine blood or *E. coli* suspension) with 5 μL of 10-mM NaOH; 2) heating to 95 °C for 1–2 min (cell lyses and inhibitory protein denaturization); 3) neutralization of basic lysate by mixing with 5 μL of 16-mM tris-HCl $(\text{pH} = 7.5)$; 4) neutralized lysate is mixed with 8–10 μL of liquid PCR reagents and primers of interest; and 5) thermal cycling. The CD fluidic design is shown schematically in Fig. 10. Three mixing channels are used in series to mix small volumes. A spinning "platen" allows control of the temperature by positioning thermoelectric devices against the appropriate fluidic chambers. The CD contacts the PC board platen on the spindle of a rotary motor, with the correct angular alignment, which is connected by a slip ring to stationary power supplies and a temperature controller. Thermocouples are used for closed-loop temperature control, and air sockets are used as insulators to isolate heating to reservoirs of interest. The thermoelectric at the PCR chamber both heats and cools and, since the PCR reaction chamber is thin (0.5 mm), fast

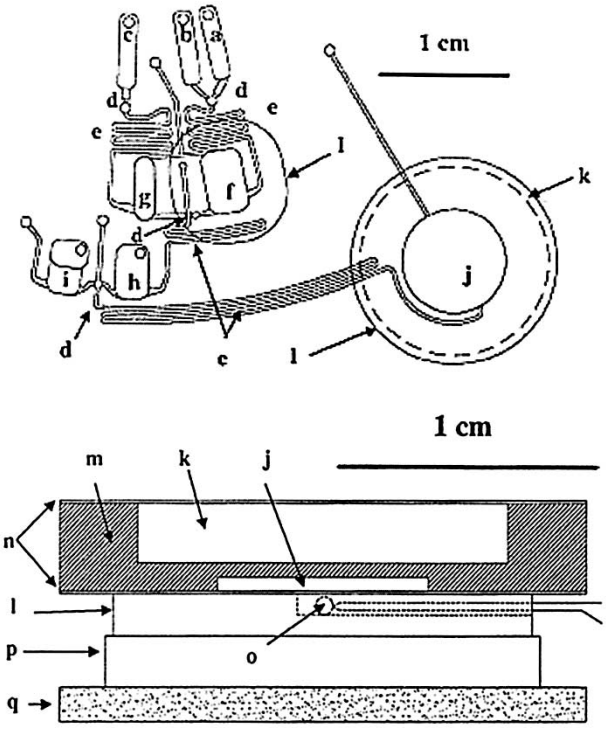

Fig. 10. Schematic illustration of the CD microfluidic PCR structure. The center of the disk is above the figure. (a) Sample. (b) NaOH (c) tris-HCL. (d) Capillary valves. (e) Mixing channels. (f) Lysis chamber. (g) tris-HCl holding chamber. (h) Neutralization lysate holding chamber. (i) PCR reagents. (j) Thermal cycling chamber. (k) Air gap. Fluids loaded in (a), (b), and (c) are driven at a first r/min into reservoirs (g) and (f), at which time (g) is heated to 95 °C. The r/min is increased and the fluids are driven into (h). The r/min is increased and fluids in (h) and (i) flow into (j). On the right, the cross section shows (m) the disk body, (k) air gap, (n) sealing layers, (l) heat sink, (p) thermoelectric, (q) PC board, and (o) thermistor. (*Proc. Micro Total Analysis Systems 2000*, © 2000, pp. 239–242, G. J. Kellogg, T. E. Arnold, B. L. Carvalho, D. C. Duffy, and N. F. Sheppard, "Centrifugal microfluidics: Applications" [22], with kind permission of Kluwer Academic Publishers.)

thermocyling is achieved. Slew rates of ± 2 Cs^{-1} with fluid volumes of 25 μL and thermal gradients across the liquid of 0.5 °C are reported. It is important to note here that the PCR chambers were not sealed; vapor generated inside the PCR chamber is condensed on the cooler surfaces of the connecting microfluidic chamber and, since the CD is rotating, the condensed drops are centrifuged back into the hot PCR chamber. This microcondensation apparatus is unique

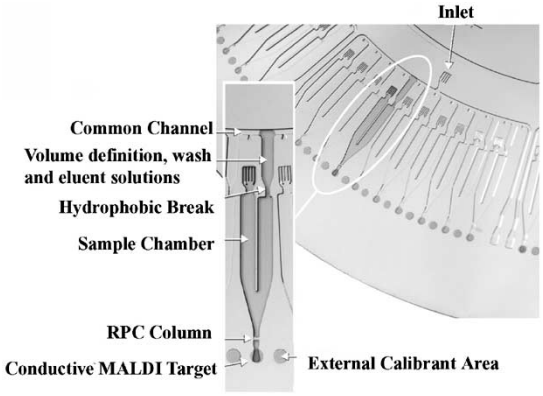

Fig. 11. Gyrolab MALDI SP1 sample preparation CD. The protein digest samples are loaded into the sample reservoir (see inset) by capillary action. Upon rotation, the sample passes through the RPC column. The peptides are bound to the column and the liquid goes out of the system into the waste. A wash buffer is loaded into the common distribution channel and volume definition chamber. The disk is rotated at a rate that will empty the common distribution channel but not allow the wash solution to pass through the hydrophobic zone. A further increase of the r/min allows the well-defined volume of wash solution to pass the hydrophobic break and wash the RPC column then be discarded as waste. Next, a well-defined volume of the elution/matrix solution is loaded and passed through the column, taking the peptides to the MALDI target zone. The flow rate is controlled to optimize the evaporation of the solvent crystallization of the protein and matrix at the target zone. (With kind permission: Application Report 101, Gyrolab MALDI SP1, Gyros AB, Uppsala, Sweden [20].)

for the centrifugal CD platform. Details of the experimental parameters used can be found in [22], but to summarize, sample preparation and PCR amplification for two types of samples, whole blood and *E. coli*, was demonstrated on the CD platform and shown to be comparable to conventional methods.

X. Sample Preparation for MALDI MS Analysis

MALDI MS peptide mapping is a commonly used method for protein identification. Correct identification and highly sensitive MS analysis require careful sample preparation. Manual sample preparation is quite tedious, time consuming, and can introduce errors common to multistep pippetting. MALDI MS sample preparation protocols employ a protein digest followed by sample concentration, purification, and recrystallization with minimal loss of protein. Automation of the sample preparation process, without sample loss or contamination, has been enabled on the CD platform by the Gyrolab MALDI SP1 CD and the Gyrolab Workstation (Gyros AB, Uppsala, Sweden) [20].

The Gyrolab MALDI SP1 sample preparation CD will process up to 96 samples simultaneously using separate microfluidic structures. Protein digest from gels or solutions are concentrated, desalted, and eluted with matrix onto a MALDI target area. The CD is then transferred to a MALDI instrument for analysis without the need for further transfer to a separate target plate. The CD fluidic structure contains functions for common reagent distribution, volume definition (metering), valving, reverse phase column (RPC) for concentration and desalting, washing, and target areas for external calibrants. Fig. 11 shows the Gyrolab MALDI SP1 sample preparation CD. The CDs are loaded with reagents and processed in a completely automated, custom workstation capable of holding up to five microtiter plates containing samples and reagents and up to five CD microlaboratories. The reagents are taken from the microplates to the CD inlets using a precision robotic arm fitted with multiple needles, the liquid is drawn into specific inlets by capillary forces, and then the needles are cleaned by rinsing at a wash station. Samples are applied in aliquots from 200 nl up to 5 μl sequentially to each channel, where it is contained using hydrophobic surface valves. The CD is then rotated, at an optimized rate, causing the sample to flow through an imbedded reverse phase chromatography column and liquid that passes through the column is collected in a waste container. Controlling the angular velocity dependent liquid flow rate maximizes protein binding to the column. A wash solution is introduced, by capillary action, into common distribution channels connected to groups of microstructures. The wash solution fills a volume definition chamber (200 nl) until it reaches a hydrophobic valve, and the CD is rotated to clear the excess liquid in the distribution channel. Not until the rotational velocity is further increased is the defined wash volume able to pass through the hydrophobic valve and into the RPC column (SOURCE 15 RPC). The peptides are eluted from the column and directly on to the MALDI target area using a solution that contains α-cyano-4-hydroxycinnamic acid and acetonitrile using the same common distribution channel and defined volume as the previous wash step. Optimization of rotational velocity during elution enables maximum recovery and balances the rate of elution with the rate of solvent evaporation from the target surface. Areas in and around the targets are gold plated to prevent charging of the surface that would cause spectral mass shift and ensures uniform field strength. Well-defined matrix/peptide crystals form in the CD MALDI target area. Gyros reports high reproducibility, high sensitivity, and improved performances when compared to conventional pipette tip technologies. Data was shown that includes comparison of 23 identical samples, processed in parallel on the same CD, from a bovine serum albumin (BSA) tryptic digest and analysis of identical samples processed on different CDs, run on different days. Sensitivities were shown in the attomole to femtomole range indicating the ability for identification of low-abundance proteins. The report attributed the superior performance of this platform to pretreatment of the CD surface to minimized nonspecific adsorption of peptides, reproducible wash volume and flow, and reproducible elution (volume, flow, and evaporation) and crystallization.

XI. Modified Commercial CD/DVD Drives in Analytical Measurements

The commercial CD/DVD drive, commonly used for data storage and retrieval, can be thought of as a laser scanning imager. The CD drive retrieves optically generated electrical

signals from the reflection of a highly focused laser light (spot size: full-width at half-maximum $\sim$1 μm), from a 1.2-mm-thick polycarbonate disk that contains a spiral optical track feature. The track is fabricated by injection molding and is composed of a series of pits that are 1–4μm long, 0.15 μm deep, and about 0.5 μm wide. The upper surface of a CD is made reflective by gold or aluminum metallization and protected with a thin plastic coating. Information is generated, as the focused laser follows the spiral track, by converting the reflected light signal into digital information. A flat surface gives a value of zero; an edge of a pit gives a value of one. The data is retrieved at a constant acquisition rate and the serial values (zero/one) are converted to data of different kinds for various applications (music, data, etc.). In addition to the code generated by the spacing of the pits, optical signals necessary for focusing, laser tracking of the spiral track, and radial position determination of the read head are monitored and used in feedback loops for proper CD operation. The laser is scanned in a radial direction toward the outer diameter of the disk with an elaborate servo that maintains both lateral tracking and vertical focusing.

Researchers [29], [30] have taken advantage of this low-cost, high-resolution optical platform in analytical DNA array applications. Barathur *et al.* [29] from Burstein Technologies, Irvine, CA, for example, have modified the normal CD drive for use as a sophisticated laser-scanning microscope for analysis of a Bio Compact Disk assay, where all analysis is carried out in microfluidic chambers on the CD. The assay is carried out concurrently with the normal optical scanning capabilities of a regular CD drive. The authors report on the application of this device for DNA micro spot-array hybridization assays and comment on its use in other diagnostic and clinical research applications. For the DNA spot-array application, arrays of capture probes for specific DNA sequences are immobilized on the surface of the CD in microfluidic chambers. Sample preparation and multiplexed PCR, using biotinylated primers, are carried out off-disk, then the biotinylated amplicons are introduced into the array chamber and hybridization occurs if amplicons with the correct sequence are present. Hybridization detection is achieved by monitoring the optical signal from the CD photo detector while the CD is rotating. To generate an optical signal when hybridization has occurred, a reporter is used; for the Bio Compact Disk assay, the reporter is a streptavidin-labeled microsphere that will bind only to the array spots which have successfully captured biotinylated amplicons. The unbound microsphere reporters are removed from the array using simple centrifugation and no further rinsing is needed. As the laser is scanned across the CD surface, the microparticle scatters light that would have normally been reflected to the photodetector, resulting in less light on the detector (bright field microscopy), and a distinctive electronic signal is generated. The electronic signal intensity data can be stored in memory then deconvoluted into an image. A 1-cm^2 microarray can be scanned in 20–30 s with a data reduction time of 5 min and custom algorithms that perform the interpretations in real time. Data was shown for identification of three different species of the *Brucella* coccobacilli on the CD platform. Human infection occurs by transmission from animals by ingestion of infected food products, contact with an infected animal, or inhalation of aerosols. Multiplex PCR-amplified DNA from all three species (common forward primers and specific reverse primers resulting in amplicons of different length for various species were used for verification of PCR on external gels) were incubated on arrays with species-specific capture probes. Removal of one of the species in the sample resulted in no probes present on that specific array spot verifying the specificity of the assay.

Alexandre *et al.* [30] at Advanced Array Technology (Namur, Belgium), utilize the inner diameter area of a CD and standard servo optics for numerical information and operational control and employ a second scanning laser system to image DNA arrays on transparent surfaces at the outer perimeter of a CD. The second laser system, consisting of a laser diode module that illuminates a 50-μm spot on the CD surface, is scanned radially at a constant linear velocity of 20 mm/min while the CD is rotating. Each CD contains 15 arrays arranged in a single ring on the CD perimeter that extends in the radial direction for 15 mm. The arrays are rectangular and consist of four rows and 11 columns of 300-μm spots. The normal CD servo optics are located below the disk and the added imaging optics are above the disk. A photodiode head follows the imaging laser and the refracted light intensity is stored digitally at a high sampling rate. An image of each array on the disk is reconstructed by deconvolution of the light intensity data. The entire CD can be scanned in less than 1 min, producing a total of 6 MB of information. Sample preparation and PCR amplification was carried out off-disk. Specific DNA capture probes were spotted on the surface of the CD using a custom arrayer that transfers the probes from a multiwell plate on to the surface of up to 12 disks using a robotic arm. Biotinylated amplicons are introduced onto the array chambers (one chamber for each array) and hybridization occurs if amplicons with the correct sequence are present. In order to get an optical signal that can be detected, after a rinse step, a solution of streptavidin-labeled colloidal gold particles is applied to the array followed by a Silver Blue solution (AAT, Namur, Belgium). The silver solution causes silver metal to grow on the gold particles thereby making the hybridization-positive micro array spots refractive to the incident laser light. Results were shown for the detection of the five most common species of *Staphylococci* and an antibiotic-resistant strain. The *fem A* and *mec A* genes of the various species of *Staphylococci* were amplified by primers common to all *Staphylococci* species then hybridized to a microarray containing spots with probes specific for the different *Staphylococci* species. The array also included a capture probe for the genus *Staphylococci* and a probe for the *mec A* gene that is associated with methicillin resistance of the *Staphylococci* species. The results were digitized and quantified with software that is part of the custom Bio-CD workstation. Signal-to-noise ratios were above 50 for all positive signals.

XII. Conclusion

In comparing miniaturized centrifugal fluidic platforms to other available micro fluid propulsion methods we have demonstrated how CD-based centrifugal methods are advantageous in many analytical situations because of their versatility in handling a wide variety of sample types, ability to gate the flow of liquids (valving), simple rotational motor requirements, ease and economic fabrication methods, and large range of flow rates attainable. Most analytical functions required for a lab on a disk, including metering, dilution, mixing, calibration, separation, etc., have all been successfully demonstrated in the laboratory. Moreover, the possibility of maintaining simultaneous and identical flow rates, to perform identical volume additions, to establish identical incubation times, mixing dynamics, and detection in a multitude of parallel CD assay elements makes the CD an attractive platform for multiple parallel assays. The platform has been commercialized by Tecan Boston for HTS [4], by Gyros AB for sample preparation techniques for MALDI [20], and by Abaxis (in a somewhat larger and less integrated rotor format compared to the CD format) for human and veterinary diagnostic blood analysis [5]. The Abaxis system for human and veterinary medicine uses only dry reagents, but for many diagnostic assays, requiring more fluidic steps, there are severe limitations in progressing toward the lab-on-a-disk goal as liquid storage on the disk becomes necessary. In HTS situations, the CD platform is being coupled to automated liquid reagent loading systems and no liquids/reagents need to be stored on the disk. The latter made the commercial introduction of the CD platform for HTS somewhat simpler [4], [20], [30]. There is an urgent need though for the development of methods for long-term reagent storage that incorporate both liquid and vapor barriers to enable the introduction of lab-on-a-disk platforms for a wide variety of fast diagnostic tests. One possible solution to this problem involves the use of lyophilized reagents with common hydration reservoir feeds, but the issue in this situation becomes the speed of the test, as the time required for redissolving the lyophilized reagents is often substantial.

The CD platform is easily adapted to optical detection methods because it is manufactured with high-optical quality plastics enabling absorption, fluorescence, and microscopy techniques. Additionally, the technology developed by the optical disk industry is being used to image the CD at the micrometer resolution, and the move to DVD and high-definition (HD) DVD will allow submicrometer resolution. The latter evolution will continue to open up new applications for the CD-based fluid platform. Whereas today the CD fluidic platform may be considered a smart microcentrifuge, we believe that in the future the integration of fluidics and informatics on the DVD and HD DVD may lead to a merging of informatics and fluidics on the same disk. One can then envision making very sharp images of the bacteria under test and correlate both test and images with library data on the disk.

Acknowledgment

The authors would like to thank S. Cresswell of Gyros AB, Uppsala, Sweden; G. J. Kellogg of Tecan Boston, Medford, MA; H. Kido and R. Barathur, Burstein Technologies, Irvine, CA; J. Lee, Ohio State University, Columbus; and M. Flynn, NASA Ames Research Center, Moffett Field, CA.

References

[1] ALPHA-MOS. [Online] Available: http://www.alpha-mos.com/newframe.htm

[2] E. V. Manz, C. S. Effenhauser, N. Burggraf, D. E. Raymond, D. J. Harrison, and H. M. Widmer, "Miniaturization of separation techniques using planar chip technology," *J. High Res. Chromatog.*, vol. 16, pp. 433–436, 1993.

[3] Caliper (home page). [Online] Available: http://www.calipertech.com/

[4] Tecan-Boston, LabCD-ADMET System. [Online] http://www.tecan-us.com/us-index.htm

[5] Abaxis (home page). [Online]. Available: http://www.abaxis.com/

[6] M. J. Madou, *Fundamentals of Microfabrication*, 2nd ed. Boca Raton, FL: CRC, 2002.

[7] S. Miyazaki, T. Kawai, and M. Araragi, "A piezo-electric pump driven by a flexural progressive wave," in *Proc. IEEE Micro Electro Mechanical Systems (MEMS'91)*, pp. 283–288.

[8] J. W. Jorgenson and E. J. Guthrie, "Liquid chromatography in open-tubular columns," *J. Chromatog.*, vol. 255, pp. 335–348, 1983.

[9] D. J. Harrison, Z. Fan, K. Fluri, and K. Seiler, "Integrated electrophoresis systems for biochemical analyses," in *Tech. Dig. 1994 Solid State Sensor and Actuator Workshop*, pp. 21–24.

[10] D. C. Duffy, H. L. Gills, J. Lin, N. F. Sheppard, and G. J. Kellogg, "Microfabicated centrifugal microfluidic systems: Characterization and multiple enzymatic assays," *Anal. Chem.*, vol. 71, no. 20, pp. 4669–4678, 1999.

[11] M. J. Madou and G. J. Kellogg, "The LabCD: A centrifuge-based microfluidic platform for diagnostics," in *Proc. SPIE Systems and Technologies for Clinical Diagnostics and Drug Discovery*, vol. 3259, G. E. Cohn and A. Katzir, Eds., 1998, pp. 80–93.

[12] G. T. A. Kovacs, *Micromachined Transducers Sourcebook*. Boston, MA: WCB/McGraw-Hill, 1998, ch. 9, pp. 787–793.

[13] G. Ekstrand, C. Holmquist, A. E. Örlefors, B. Hellman, A. Larsson, and P. Anderson, "Microfluidics in a Rotating CD," in *Proc. Micro Total Analysis Systems 2000*, A. van den Berg, W. Olthuis, and P. Bergveld, Eds., pp. 311–314.

[14] A.-L. Tiensuu, O. Öhman, L. Lundbladh, and O. Larsson, "Hydrophobic valves by ink-jet printing on plastic CD's with integrated microfluidics," in *Proc. Micro Total Analysis Systems 2000*, A. van den Berg, W. Olthuis, and P. Bergveld, Eds., pp. 575–578.

[15] M. J. Madou, Y. Lu, S. Lai, J. Lee, and S. Daunert, "A centrifugal microfluidic platform—A comparison," in *Proc. Micro Total Analysis Systems 2000*, A. van den Berg, W. Olthuis, and P. Bergveld, Eds., 2000, pp. 565–570.

[16] J. Zeng, D. Banerjee, M. Deshpande, J. R. Gilbert, D. C. Duffy, and G. J. Kellogg, "Design analysis of capillary burst valves in centrifugal microfluidics," in *Proc. Micro Total Analysis Systems 2000*, A. van den Berg, W. Olthuis, and P. Bergveld, Eds., pp. 579–582.

[17] I. H. A. Badr, R. D. Johnson, M. J. Madou, and L. G. Bachas, "Fluorescent ion-selective optode membranes incorporated onto a centrifugal microfluidics platform," *Anal. Chem.*, vol. 74, no. 21, pp. 5569–5575, Nov. 2002.

[18] R. D. Johnson, I. H. A. Badr, G. Barrett, S. Lai, Y. Lu, M. J. Madou, and L. G. Bachas, "Development of a fully integrated analysis system for ions based on ion-selective optodes and centrifugal microfluidics," *Anal. Chem.*, vol. 73, no. 16, pp. 3940–3946, Aug. 2001.

[19] M. McNeely, M. Spute, N. Tusneem, and A. Oliphant, "Hydrophobic microfluidics," in *Proc. Microfluidic Devices and Systems*, vol. 3877, 1999, pp. 210–220.

[20] "Application Report 101, Gyrolab MALDI SP1," Gyros US, Inc., Monmouth Junction, NJ.

[21] S. Lai, S. Wang, J. Luo, J. Lee, S. Yang, and M. J. Madou, "Compact disc (CD) platform for enzyme-linked immunosorbant assays," *Anal. Chem.*, submitted for publication.

[22] G. J. Kellogg, T. E. Arnold, B. L. Carvalho, D. C. Duffy, and N. F. Sheppard, "Centrifugal microfluidics: Applications," in *Proc. Micro Total Analysis Systems 2000*, A. van den Berg, W. Olthuis, and P. Bergveld, Eds., pp. 239–242.

[23] N. Thomas, A. Ocklind, I. Blikstad, S. Griffiths, M. Kenrick, H. Derand, G. Ekstrand, C. Ellström, A. Larsson, and P. Anderson, "Integrated cell based assays in microfabricated disposable CD devices," in *Proc. Micro Total Analysis Systems 2000*, A. van den Berg, W. Olthuis, and P. Bergveld, Eds., pp. 249–252.

[24] A. W. Anderson, *Physical Chemistry of Surfaces*. New York: Wiley, 1960, ch. 1, pp. 5–6.
[25] G. J. Kellogg, private communication.
[26] D. C. Duffy, J. C. McDonald, O. J. A. Schueller, and G. M. Whitesides, "Rapid prototyping of microfluidic systems in poly(dimethylsiloxane)," *Anal. Chem.*, vol. 70, pp. 4974–4984, 1998.
[27] J. Burbaum, "Minitaturization technologies in HTS: How fast, how small, how soon?," *Drug Discovery Today*, vol. 3, no. 7, pp. 313–312, 1998.
[28] J. V. Zoval, R. Boulanger, C. Blackwell, B. Borchers, M. Flynn, D. Smernoff, R. Landheim, R. Mancinelli, and M. J. Madou, Cell viability assay on a rotating disc analytical system. In preparation.
[29] R. Barathur, J. Bookout, S. Sreevatsan, J. Gordon, M. Werner, G. Thor, and M. Worthington, "New disc-based technologies for diagnostic and research applications," *Psych. Genetics*, vol. 12, no. 4, pp. 193–206, 2002.
[30] I. Alexandre, Y. Houbion, J. Collet, S. Hamels, J. Demarteau, J.-L. Gala, and J. Remacle, "Compact disc with both numeric and genomic information as DNA microarray platform," *BioTechniques*, vol. 33, no. 2, p. 435, 2002.

Jim V. Zoval received the Ph.D. degree in physical chemistry from the University of California, Irvine, in 1996.

He is currently a Faculty Specialist in the Department of Mechanical and Aerospace Engineering at the University of California, Irvine. He has six years of industrial experience in clinical and medical diagnostic platform development. His research interests are in nanotechnology, molecular biology, biochemistry, nanobiotechnology, electrochemistry, sensors/biosensors, optical microscopy, electronic microscopy, scanning probe microscopy, and spectroscopy.

Marc J. Madou received the B.Sc. and M.Sc. degrees in physical chemistry from Rijksuniversiteit, Ghent, Belgium, in 1973 and 1975, respectively. He received the Ph.D. degree (*summa cum laude*) in semiconductor electrochemistry from the Solid State Physics Laboratory, Rijksuniversiteit, in 1978. His Ph.D. dissertation was on n- and p-type GaP as semiconductor electrodes.

He was Vice President of Advanced Technology, Nanogen, San Diego, CA. He was also the Founder of the Microsensor Department, SRI International, Menlo Park, CA, Founder and President of Teknekron Sensor Development Corporation (TSDC), Menlo Park, CA, Visiting Miller Professor at the University of California, Berkeley, and Endowed Chair (Professor in Chemistry and Materials Science and Engineering) at Ohio State University, Columbus. He is currently Chancellor's Professor in the Department of Mechanical and Aerospace Engineering, University of California, Irvine. He specializes in the application of miniaturization technology to chemical and biological problems (bioMEMS). He is the author of more than 100 peer-reviewed papers and has written several books in this burgeoning field he helped pioneer both in Academia and in Industry. The second edition of his *Fundamentals of Microfabrication* (Boca Raton, FL: CRC, 2002), an introduction to MEMS, has become known as the bible of micromachining; he is now at work on the third edition. He is also the Editor of *Sensors and Actuators B* (North and South America). His recent research work involves artificial muscle for responsive drug delivery, DNA arrays, carbon-MEMS, a compact disk-based fluidic platform, protein-based actuators, a compact disc-based fluidic platform, and a solid-state pH electrode based on IrOx.